

# Step-by-step growth of epitaxially aligned polythiophene by surface-confined reaction

J. A. Lipton-Duffin<sup>a,b</sup>, J. A. Miwa<sup>a,b</sup>, M. Kondratenko<sup>b,c</sup>, F. Cicoira<sup>a,b</sup>, B. G. Sumpter<sup>d</sup>, V. Meunier<sup>d,1</sup>, D. F. Perepichka<sup>b,c,1</sup>, and F. Rosei<sup>a,b,1</sup>

<sup>a</sup>Institut National de Recherche Scientifique – Énergie, Matériaux et Télécommunications, Université du Québec, 1650 Boulevard Lionel-Boulet, Varennes, QC, Canada J3X 1S2; <sup>b</sup>Center for Self-Assembled Chemical Structures and <sup>c</sup>Department of Chemistry, McGill University, 801 Sherbrooke Street West, Montréal, QC, Canada H3A 2K6; and <sup>d</sup>Oak Ridge National Laboratory, P.O. Box 2008 MS6367, Oak Ridge, TN 37831-6367

Edited by Nicholas J. Turro, Columbia University, New York, NY, and approved May 11, 2010 (received for review January 20, 2010)

**One of the great challenges in surface chemistry is to assemble aromatic building blocks into ordered structures that are mechanically robust and electronically interlinked—i.e., are held together by covalent bonds. We demonstrate the surface-confined growth of ordered arrays of poly(3,4-ethylenedioxythiophene) (PEDOT) chains, by using the substrate (the 110 facet of copper) simultaneously as template and catalyst for polymerization. Copper acts as promoter for the Ullmann coupling reaction, whereas the inherent anisotropy of the fcc 110 facet confines growth to a single dimension. High resolution scanning tunneling microscopy performed under ultrahigh vacuum conditions allows us to simultaneously image PEDOT oligomers and the copper lattice with atomic resolution. Density functional theory calculations confirm an unexpected adsorption geometry of the PEDOT oligomers, which stand on the sulfur atom of the thiophene ring rather than lying flat. This polymerization approach can be extended to many other halogen-terminated molecules to produce epitaxially aligned conjugated polymers. Such systems might be of central importance to develop future electronic and optoelectronic devices with high quality active materials, besides representing model systems for basic science investigations.**

metal-catalyzed coupling reaction | molecular wires | *cis*-polythiophene | scanning probe microscopy | polymerization mechanism

The tunability and diversity of the structural and electronic properties of  $\pi$ -conjugated organic polymers have spurred a wide interest in these materials as wires and semiconductors for future electronic devices (1, 2), although significant optimization is required for real breakthrough performance. Conventional organic synthesis can create conjugated polymers of practically any length and structure (3), yet their controlled positioning and ordering on a surface remains nontrivial. This supramolecular ordering ultimately controls properties such as the charge mobility and recombination, which are critical for any application, including nanoelectronics and light harvesting. The approach presented here proposes a way to precisely control the long-range order in conducting polymers by performing synthesis of these materials, in an epitaxial way, directly on crystalline substrates. Although electrochemical polymerization on conducting surfaces has long been used to prepare films of conjugated polymers such as polythiophene (4), the techniques for preparation and characterization of aligned arrays of polymers have only recently been developed. Promising results were obtained by using UV irradiation (5) or scanning probe microscope tip pulsing (6) to form polydiacetylenes and surface-catalyzed coupling to form polyphenylene (7). However, these polymers are not good conductors due to a very large bond length alternation in their conjugated acetylene structures. (8). Conductive ordered polythiophene wires have been prepared by pulsed electrooxidative polymerization of substituted thiophenes (9, 10). The symmetry of the Au(111)/I<sub>2</sub> used in these experiments led to preferential polymer growth along one of the three equivalent crystallographic axes. However, the linear structure of those polymers was perturbed by the kinks

induced by occasional *cis*-conformation of thiophene-thiophene links, and no extended ordered polymer domains were observed.

Poly(3,4-ethylenedioxythiophene) (PEDOT) is the most industrially important conducting polymer (4, 11), because of its combined characteristics of high electrical conductivity, high transparency, and exceptional stability in its doped (conducting) state. It is widely used in the fabrication of electroactive devices (12), in particular for organic light-emitting diodes and photovoltaic cells, as well as sensors, electrochromics, and as an oxygen reduction catalyst (13). There has been a significant interest in using PEDOT in nanoelectronic devices although existing methods for preparing nanostructured PEDOT materials are limited to relatively large structures lacking molecular order (14–16). Here we report a surface-confined synthesis of PEDOT delivering an epitaxially confined array of oligomer wires; we demonstrate control over the chain length and identify a surprising conformational structure (*cis*-PEDOT), which is strikingly different from *anti*-PEDOT synthesized by conventional techniques. To prepare this material, we exploited the Ullmann coupling (17–19) reaction, which is the oldest known method for C-C coupling of aromatic halides (though its application to the synthesis of conjugated polymers has been very limited so far). Specifically, we synthesized the epitaxially aligned PEDOT by using an atomically flat Cu(110) surface as a substrate and as a promoter for the polymerization reaction of 2,5-diiodo-3,4-ethylenedioxythiophene (DIEDOT). We obtained similar results by using 2,5-dibromo-3,4-ethylenedioxythiophene. The very high resolution of scanning tunneling microscopy (STM) under atomically clean ultrahigh vacuum (UHV) conditions combined with density functional theory (DFT) calculations allowed us to illustrate mechanistic details of the polymerization, which leads to the *cis*-PEDOT conformational structure.

In this paper we show that strong molecule–copper interactions are the main factor limiting the length of the produced oligomers. We further observe that the same interactions allow us to produce conjugated polythiophene of an otherwise inaccessible geometry (*all-cis*). This synthesis method also solves two critical problems associated with controlling the nanostructure of the polymer: We can reliably produce a single layer of polymer exclusively at the surface and additionally make use of the inherent anisotropy of the (110) facet as a means of templating the growth in a single direction. The approach can be easily extended to other aromatic

Author contributions: D.F.P. and F.R. designed research; J.A.L.-D., J.A.M., M.K., F.C., B.G.S., and V.M. performed research; J.A.L.-D., B.G.S., and V.M. analyzed data; and J.A.L.-D., V.M., D.F.P., and F.R. wrote the paper.

The authors declare no conflict of interest.

This article is a PNAS Direct Submission.

Freely available online through the PNAS open access option.

<sup>1</sup>To whom correspondence should be addressed. E-mail: meunierv@ornl.gov, dmitrii.perepichka@mcgill.ca, or rosei@emt.inrs.ca.

This article contains supporting information online at [www.pnas.org/lookup/suppl/doi:10.1073/pnas.1000726107/-DCSupplemental](http://www.pnas.org/lookup/suppl/doi:10.1073/pnas.1000726107/-DCSupplemental).

halides and is not limited to copper: Pd, Ag, and Ni could also be used as catalysts for this reaction (20).

## Results

Dosing DIEDOT on a Cu(110) surface held at 200 °C produces a sparse array of lines oriented along the [1–10] direction of the Cu lattice, separated by the Cu(110)-(1 × 1) lattice, as shown in the STM micrograph displayed in Fig. 1A. In this coverage regime we are routinely able to image both the molecular features and the atomic lattice simultaneously. The elements of the molecular lines are found to be spaced by 5.12 Å, which is double the nearest-neighbor spacing along the [1–10] direction (2.56 Å). This spacing is substantially larger than the expected 3.963 Å internal spacing of PEDOT (21), and thus we conclude that the molecules are not covalently bonded to one another. A lattice fitted to the adjacent bare substrate demonstrates that the molecules in Fig. 1 occupy long bridge sites. The dehalogenation of the molecules is confirmed by X-ray photoelectron spectroscopy (XPS) (*SI Text*) although the usual ordered iodine-*c*(2 × 2) overlayer (22) is not observed until a critical coverage is achieved (see below). We thus conclude that these lines comprise individual EDOT moieties, bonded to the substrate but not to each other. Their alignment is attributed to the cumulative effects of the substrate anisotropy and the weakly attractive van der Waals interactions between the ethylenedioxy moieties.

Structures calculated by DFT and shown in Fig. 1B and C indicate that the dehalogenated molecules are oriented with the sulfur atoms pointing toward the surface. As was observed in the experimental data, the molecules reside above the long bridge sites of the Cu(110) lattice, because this corresponds to the lowest energy adsorption site identified by DFT. The model

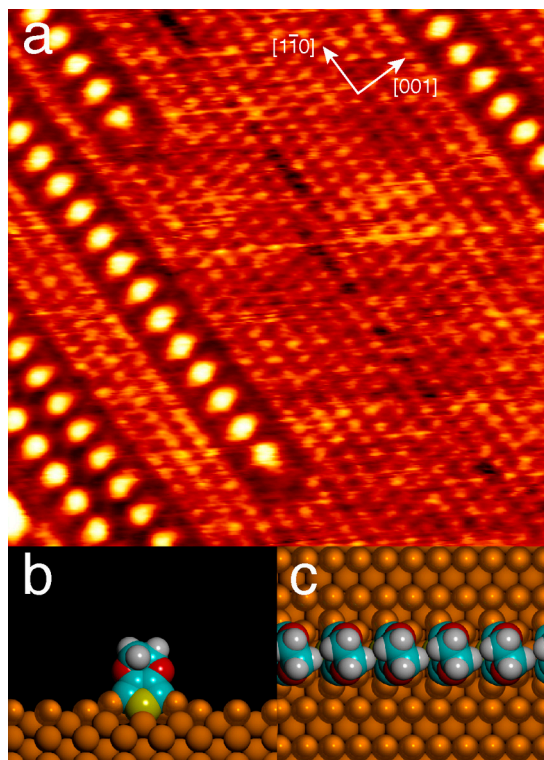


**Fig. 1.** Low-coverage of EDOT monomers on Cu(110) self-organize into stacks. (A) STM image showing stacks of EDOT molecules on Cu(110) subsequent to a five-minute DIEDOT exposure [ $V = -365$  mV,  $I = 1.0$  nA,  $(8.9 \text{ nm})^2$ ]. The surrounding bare regions of the Cu(110) substrate exhibit a  $(1 \times 1)$  symmetry. The positions of the molecules in the stack are shown, as calculated by DFT viewed from (B) the front and (C) the top. The model shows Cu atoms lifted out of the top substrate layer to participate in bonding to the EDOT.

shows that each molecule is tilted by approximately 18° away from the surface normal toward the [1–10] direction. The mostly upright orientation is somewhat surprising for thiophene-derived units. Flat or slightly tilted orientations, enabling aromatic–metal interactions, have been consistently observed for oligothiophenes on Ag (23), Au (24, 25), and Cu(110) (26, 27). The upright orientation for dehalogenated EDOT is stabilized by two C–Cu bonds, as well as by strong Cu–S interactions and weak van der Waals contacts with the adjacent molecules in the stack. This binding leads to an adsorption energy of 5.38 eV, which is much larger than the adsorption energy of the thiophene  $\text{C}_4\text{H}_4\text{S}$  on Cu(110) (0.50 eV), which adsorbs in a virtually planar orientation (28). This strong binding to the surface and the large separation between the monomers (5.12 Å) prevents polymerization along the [1–10] direction.

With increasing DIEDOT deposition, the density of the lines increases, and adjacent lines begin to bond perpendicularly in the [001] direction. The higher the DIEDOT coverage, the more adjacent lines are bonded, forming dimers, trimers, and so on, as shown in Fig. 2A, where several oligomers of various lengths are observed, surrounded by a brighter second layer species in a  $c(2 \times 2)$  configuration (see below). This observation implies that the bonded thiophene units must all be oriented in the same manner (*cis*), with the sulfur atoms pointing toward the surface, in striking contrast to the usual EDOT dimer and polymer *anti*-geometry (21). Thus the Cu–S interaction is maintained even when dimers are formed, and Fig. 2C demonstrates the extension of the dimer growth mode to the trimer geometry. In the trimers the center unit appears brighter than the outer two in the STM image, and, likewise, the outer two units of tetramers are dimmer than the central ones (see *SI Text*), suggesting the arched geometry proposed in the models, where the end units of each chain are tilted with respect to the surface normal, but the central ones remain erect and are lifted away from the surface. The growth process is depicted in Fig. 3. Dehalogenation of the monomer is the fastest step and readily occurs even at room temperature (7). The chain growth is then controlled by coupling of the Cu-bonded dehalogenated EDOT intermediates. The DFT calculations suggest that production of oligomers of unbounded length is limited by inner units being shifted away from the substrate, thereby reducing the stabilizing Cu–S interaction. Indeed, the corresponding adsorption energies (5.92 eV for dimer, 7.58 eV for trimer, and 8.11 eV for tetramer) show a clear tendency toward saturation. The presence of a majority of dimers, trimers, etc., at given coverages suggests a competition between the compressive strain internal to the oligomers and the energy gained by the bonding. As the surface coverage is increased, the energy gain for forming longer structures balances the strain energy, whereas this effect is not observed at low coverages where only single monomer stacks are found. The distribution of these structures is examined in *SI Text*.

Higher coverage of DIEDOT produces a surface that is completely saturated with alternating stripes of PEDOT oligomers and *I-c*(2 × 2), as shown in Fig. 4. Chains up to 14 units long are formed and define a  $p(1 \times 2)$  lattice, as shown by the green rectangle (see also *SI Text*). The average distance between EDOT-EDOT elements along the [1–10] direction is measured to be  $3.57 \pm 0.04$  Å, which is consistent with the Cu(110) lattice constant (3.61 Å). These distances are ~10% smaller than the gas-phase EDOT-EDOT separation of 3.963 Å (21) expected for the free polymer (which adopts an all-*anti* conformation in the gas phase). This spacing is attributed to the strain induced by the strong polymer–Cu interaction. The measured center-to-center spacing of the chain elements implies a (C2...C5) spacing of neighboring units of less than 2 Å, which is only compatible with the formation of a covalent bond. This hypothesis of covalent bonding is further supported by the apparent delocalization of



Polymerization is controlled by the classical Ullmann dissociative coupling mechanism, in which the substrate itself acts as a catalyst, thus suggesting a general approach for this type of reaction. We expect that this method will be particularly useful in the controlled growth of unique 2D conjugated structures, which are currently the focus of widespread research (29–35).

## Materials and Methods

A single crystal (110) oriented Cu specimen was cleaned by repeated cycles of ion bombardment ( $\text{Ar}^+$  at 600 eV) and annealing to  $\approx 800$  K. The DIEDOT was synthesized as described before (36). For evaporation, a sample of DIEDOT was located outside the main UHV system in an evacuated vial and was dosed into the vacuum chamber through a drift tube. The DIEDOT sample and dosing lines were heated to 100 °C to increase the deposition rate. Line of sight to the sample from the drift tube was necessary for appreciable accumulation over several minutes of dosing. During and subsequent to dosing, we heated the substrate to 200 °C to accelerate the dehalogenation reaction and promote growth through increased surface mobility of the free monomers. All measurements were collected by using a commercial UHV system with a variable temperature scanning tunneling microscope (Omicron GmbH). The bias voltages are quoted from the tip to the sample. The system has a base pressure of  $< 2 \times 10^{-11}$  mbar. Unless stated otherwise the sizes measured by the STM are accurate to within 5% of the quoted values, with the uncertainties arising from thermal drift and/or piezo creep. The data have been corrected to reflect the known lattice spacing of bare Cu(110), or of the Cu(110) 1-c( $2 \times 2$ ) reconstruction, where appropriate. All image analysis was performed by using the free WSxM software (37), with analyses typically involving plane flattening and smoothing to enhance critical details, as well as distortion correction to compensate for instrument drift.

Theoretical modeling [including energetics, relaxation of the atomistic models for the various polymers on Cu (110) surface, and image simulation] was based on DFT, using the VASP package (38–40). The calculations were

carried out by using a slab model keeping the atoms of the bottom layers at bulk positions to simulate the semiinfinite crystal. The unit cell for most of the calculations had a lateral dimension of  $0.497 \times 2.81$  nm<sup>2</sup>, representing a 2 (along [1–10])  $\times$  8 (along [001]) unit cell in the plane. The slab was made up of five layers, because it was determined that the results do not quantitatively change by increasing the slab size to eight layers. In the direction perpendicular to the slab, the cell dimension was chosen to ensure a 1.80-nm vacuum between periodic images. Core atomic states were represented by projector augmented wave pseudopotentials (41, 42) within the local density approximation for the exchange-correlation functional (43). Numerical convergence was ensured by using a plane-wave basis cutoff of 400 eV and a  $8 \times 2 \times 1$  Monkhorst–Pack grid (corresponding to eight independent  $k$  points) to sample the surface Brillouin zone (44). For each structure, energy convergence down to 0.1 meV and forces smaller than 1 meV/Å were systematically reached. The STM simulations (*SI Text*) were performed by using the converged wave functions from the DFT runs and within the Tersoff–Hamann approximation (45) as implemented in the BSKAN package (46).

**ACKNOWLEDGMENTS.** The authors are grateful to G. Contini and J.M. MacLeod for critical readings of the manuscript. This research was funded by Natural Sciences and Engineering Research Council of Canada, Air Force Office of Scientific Research and Asian Office of Aerospace Research and Development of the USA, the Petroleum Research Fund of the American Chemical Society, and Ministère du Développement économique, de l'Innovation et de l'Exportation of Quebec. We also acknowledge support from the Fonds québécois de la recherche sur la nature et les technologies Centre for Self-Assembled Chemical Structures, a DuPont Young Professor Award (D.F.P.), and the Canada Research Chairs program (F.R.). V.M. and B.G.S. were supported by the Center for Nanophase Materials Sciences, sponsored by the Division of Scientific User Facilities, US Department of Energy and in part through the Polymer-Based Materials for Harvesting Solar Energy, an Energy Frontier Research Center funded by the US Department of Energy, Office of Science, Office of Basic Energy Sciences under Award Number DE-SC0001087.

- Nitzan A, Ratner MA (2003) Electron transport in molecular wire junctions. *Science* 300(5624):1384–1389.
- Magoga M, Joachim C (1997) Conductance and transparency of long molecular wires. *Phys Rev B* 56(8):4722–4729.
- Tour JM (1996) Conjugated macromolecules of precise length and constitution. Organic synthesis for the construction of nanoarchitectures. *Chem Rev* 96(1):537–553.
- Groenendaal L, Zotti G, Aubert PH, Waybright SM, Reynolds JR (2003) Electrochemistry of poly(3,4-alkylenedioxythiophene) derivatives. *Adv Mater* 15(11):855–879.
- Grim PCM, et al. (1997) Submolecularly resolved polymerization of diacetylene molecules on the graphite surface observed with scanning tunneling microscopy. *Angew Chem Int Ed* 36(23):2601–2603.
- Okawa Y, Aono M (2001) Materials science—Nanoscale control of chain polymerization. *Nature* 409(6821):683–684.
- Lipton-Duffin JA, Ivasenko O, Perepichka DF, Rosei F (2009) Synthesis of polyphenylene molecular wires by surface-confined polymerization. *Small* 5(5):592–597.
- Akai-Kasaya M, et al. (2003) Electronic structure of a polydiacetylene nanowire fabricated on highly ordered pyrolytic graphite. *Phys Rev Lett* 91(25):255501.
- Sakaguchi H, Matsumura H, Gong H, Abouelwafa AM (2005) Direct visualization of the formation of single-molecule conjugated copolymers. *Science* 310(5750):1002–1006.
- Sakaguchi H, Matsumura H, Gong H (2004) Electrochemical epitaxial polymerization of single-molecular wires. *Nat Mater* 3(8):551–557.
- Groenendaal BL, Jonas F, Freitag D, Pielartzik H, Reynolds JR (2000) Poly(3,4-ethylenedioxythiophene) and its derivatives: Past, present, and future. *Adv Mater* 12(7):481–494.
- Kirchmeyer S, Reuter K (2005) Scientific importance, properties and growing applications of poly(3,4-ethylenedioxythiophene). *J Mater Chem* 15(21):2077–2088.
- Winther-Jensen B, Winther-Jensen O, Forsyth M, MacFarlane DR (2008) High rates of oxygen reduction over a vapor phase-polymerized PEDOT electrode. *Science* 321(5889):671–674.
- Chen YX, Luo Y (2009) Precisely defined heterogeneous conducting polymer nanowire arrays—Fabrication and chemical sensing applications. *Adv Mater* 21(20):2040–2044.
- Hamed M, Herland A, Karlsson RH, Inganäs O (2008) Electrochemical devices made from conducting nanowire networks self-assembled from amyloid fibrils and alkoxy-sulfonate PEDOT. *Nano Lett* 8(6):1736–1740.
- Xiao R, Il Cho S, Liu R, Lee SB (2007) Controlled electrochemical synthesis of conductive polymer nanotube structures. *J Am Chem Soc* 129(14):4483–4489.
- Ullmann F, Bielecki J (1901) Synthesis in the Biphenyl series. (I. Announcement). *Ber Deutsch Chem Ges* 34:2174–2185.
- Xi M, Bent BE (1993) Mechanisms of the Ullmann coupling reaction in adsorbed monolayers. *J Am Chem Soc* 115(16):7426–7433.
- Hassan J, Seignion M, Gozzi C, Schulz E, Lemaire M (2002) Aryl-aryl bond formation one century after the discovery of the Ullmann reaction. *Chem Rev* 102(5):1359–1469.
- Gutzler R, et al. (2009) Surface mediated synthesis of 2D covalent organic frameworks: 1,3,5-tris(4-bromophenyl)benzene on graphite(001), Cu(111), and Ag(110). *Chem Commun* 4456–4458.
- Kim EG, Bredas JL (2008) Electronic evolution of poly(3,4-ethylenedioxythiophene) (PEDOT): From the isolated chain to the pristine and heavily doped crystals. *J Am Chem Soc* 130(50):16880–16889.
- Andryushechkin BV, Eltsov KN, Shevlyuga VM (2005) Atomic structure of chemisorbed iodine layer on Cu(110). *Surf Sci* 584(2–3):278–286.
- Yoshikawa G, Kiguchi M, Ikeda S, Saiki K (2004) Molecular orientations and adsorption structures of alpha-sexithienyl thin films grown on Ag(110) and Ag(111) surfaces. *Surf Sci* 559(2–3):77–84.
- Glowatzki H, Duhm S, Braun KF, Rabe JP, Koch N (2007) Molecular chains and carpets of sexithiophenes on Au(111). *Phys Rev B* 76(12):125425.
- Kiel M, Duncker K, Hagendorf C, Widdra W (2007) Molecular structure and chiral separation in alpha-sexithiophene ultrathin films on Au(111): Low-energy electron diffraction and scanning tunneling microscopy. *Phys Rev B* 75(19):195439.
- Kiguchi M, Yoshikawa G, Ikeda S, Saiki K (2004) Molecular orientation control of sexithienyl thin film on Cu substrates. *Surf Sci* 566–568(Part 1):603–607.
- Oehzelt M, et al. (2009) alpha-Sexithiophene on Cu(110) and Cu(110)-(2 x 1)O: An STM and NEXAFS study. *Surf Sci* 603(2):412–418.
- Sony P, Puschnig P, Nabok D, Ambrosch-Draxl C (2007) Importance of van der Waals interaction for organic molecule-metal junctions: Adsorption of thiophene on Cu(110) as a prototype. *Phys Rev Lett* 99(17):176401.
- Gourdon A (2008) On-surface covalent coupling in ultrahigh vacuum. *Angew Chem Int Ed* 47(37):6950–6953.
- Perepichka DF, Rosei F (2009) Extending polymer conjugation into the second dimension. *Science* 323:216–217.
- Sakamoto J, van Heijst J, Lukin O, Schluter AD (2009) Two-dimensional polymers: Just a dream of synthetic chemists? *Angew Chem Int Ed* 48(6):1030–1069.
- Grill L, et al. (2007) Nano-architectures by covalent assembly of molecular building blocks. *Nat Nanotech* 2(11):687–691.
- Veld ML, Iavicoli P, Haq S, Amabilino DB, Raval R (2008) Unique intermolecular reaction of simple porphyrins at a metal surface gives covalent nanostructures. *Chem Commun* 13:1536–1538.
- Weigelt S, et al. (2007) Covalent interlinking of an aldehyde and an amine on a Au (111) surface in ultrahigh vacuum. *Angew Chem Int Ed* 46(48):9227–9230.
- Bieri M, et al. (2009) Porous graphenes: Two-dimensional polymer synthesis with atomic precision. *Chem Commun* 6919–6921.
- Meng H, et al. (2003) Solid-state synthesis of a conducting polythiophene via an unprecedented heterocyclic coupling reaction. *J Am Chem Soc* 125(49):15151–15162.
- Horcas I, et al. (2007) WSxM: A software for scanning probe microscopy and a tool for nanotechnology. *Rev Sci Instrum* 78(1):013705.
- Kresse G, Furthmüller J (1996) Efficient iterative schemes for ab initio total-energy calculations using a plane-wave basis set. *Phys Rev B* 54(16):11169–11186.
- Kresse G, Furthmüller J (1996) Efficiency of ab-initio total energy calculations for metals and semiconductors using a plane-wave basis set. *Comp Mater Sci* 6(1):15–50.
- Kresse G, Hafner J (1993) Abinitio molecular-dynamics for liquid-metals. *Phys Rev B* 47(1):558–561.
- Blöchl PE (1994) Projector augmented-wave method. *Phys Rev B* 50(24):17953–17979.

42. Kresse G, Joubert D (1999) From ultrasoft pseudopotentials to the projector augmented-wave method. *Phys Rev B* 59(3):1758–1775.
43. Ceperley DM, Alder BJ (1980) Ground-state of the electron-gas by a stochastic method. *Phys Rev Lett* 45(7):566–569.
44. Monkhorst HJ, Pack JD (1976) Special points for Brillouin-zone integrations. *Phys Rev B* 13(12):5188–5192.
45. Tersoff J, Hamann DR (1985) Theory of the scanning tunneling microscope. *Phys Rev B* 31(2):805–813.
46. Hofer WA, Redinger J (2000) Scanning tunneling microscopy of binary alloys: First principles calculation of the current for PtX (100) surfaces. *Surf Sci* 447(1–3):51–61.